https://doi.org/10.1016/j.sse.2017.07.008

This is the Pre-Published Version.

Enhanced Tunability of Electrical and Magnetic Properties in (La,Sr)MnO_3 Thin Films via Field-assisted Oxygen Vacancy Modulation

H.F. Wong[1], S.M. Ng[1], W. F. Cheng[1], Y.K. Liu[1], X.X. Chen[1], D. von Nordheim[2], C.L. Mak[1], J.Y. Dai[1] , B. Ploss[2] and C.W. Leung[1,*]

[1] Department of Applied Physics, The Hong Kong Polytechnic University, Hung Hom, Kowloon, Hong Kong

[2] Department of SciTec, University of Applied Sciences Jena, Carl-Zeiss-Promenade 2, 07743 Jena, Germany

* Tel: +852 27665670, Fax: +852 23337629, Email: dennis.leung@polyu.edu.hk

© 2017. This manuscript version is made available under the CC-BY-NC-ND 4.0 license https://creativecommons.org/licenses/by-nc-nd/4.0/

Abstract

We have investigated the tunability of the transport and magnetic properties in 7.5 nm $La_{0.7}Sr_{0.3}MnO_3$ (LSMO) epitaxial films in a field effect geometry with the ferroelectric copolymer P(VDF-TrFE) as the gate insulator. Two different switching behaviors were observed upon application of gate voltages with either high or low magnitudes. The application of single voltage pulses of alternating polarity with an amplitude high enough to switch the remnant polarization of the ferroelectric copolymer led to a 15 % change of the resistance of the LSMO channel at temperature 300 K (but less than 1 % change at 20 K). A minimal shift of the peak in the resistance-temperature plot was observed, implying that the Curie temperature T_C of the manganite layer is not changed. Alternatively, the application of a chain of low voltage pulses was found to shift T_C by more than 14 K, and a change of the channel resistance by a 45 % was obtained. We attribute this effect to the field-assisted injection and removal of oxygen vacancies in the LSMO layer, which can occur across the thickness of the oxide film. By controlling the oxygen migration, the low-field switching route offers a simple method for modulating the electric and magnetic properties of manganite films

Keywords: LSMO, Voltage Control Magnetism, Ferroelectric, pulse chains

Introduction

With the scaling down of non-volatile memory devices, power management has become one of the most pressing challenges for the semiconductor industry. For example, significant improvement was made to reduce the current density of spin-transfer torque magnetic random access memory (STT-MRAM) devices[1]. Besides using an electric current, the manipulation of the magnetic properties by an electric field can further reduce the power consumption. The manipulation of magnetism via an electric field has therefore attracted much attention[2-4]. Recent progress has successfully demonstrated the control of saturation magnetization[5-7], Curie temperature[5, 7-10], magnetic anisotropy[5, 7, 11] and exchange bias in magnetic thin films[5, 12] or heterostructures[5, 13, 14].

Manipulating the magnetic properties in ferromagnets (FM) via an electric field can be classified into two approaches. The first approach relies on the magnetoelectric (ME) coupling between ferroelectric (FE) and magnetic order in a single phase multiferroic, which is promising for future multifunctional devices[2, 12]. Unfortunately, only a few systems demonstrate the coexistence of FE and FM[12, 15]. Alternatively, artificial multiferroic heterostructures were also deployed to achieve the manipulation of magnetism via an electric field[16]. Such heterostructures consist of a FM that is gated with FE oxides. Based on the polarization reversal in the FE oxides, carriers in the FM film are attracted towards (or repelled from) the FM/FE interfaces. This electrostatic effect induces changes in the carrier concentration in the FM, accompanied by a change of the magnetic properties. However, FM metals have high carrier concentrations (10^{21} - 10^{22} cm^{-3}), resulting in a very short electrostatic screening depth, and ultra-thin FM layers are therefore required[16]. In general, for achieving high microstructural match quality between the FM and FE materials, epitaxial growth of FM and FE materials is required. For example, $Pb_x Zr_{1-x}TiO_3$ and $BaTiO_3$ are

promising candidates due to their high FE polarization coefficients and compatibility with various FM oxides[4, 17, 18].

For high compatibility with different epitaxial FM oxide, FE polymers such as the copolymer of polyvinylidene fluoride with trifluoroethylene P(VDF-TrFE) have attracted much attention due to their unique properties. They are lead-free, they have a high-flexibility and the highest dielectric constant (κ ~10) among other FE polymer[19, 20]. Stolichnov et al. used P(VDF-TrFE) as a FE layer to control the ferromagnetism (Curie temperature and coercive field) in (Ga,Mn)As[21].

The second approach for electrical modulation of magnetism is to induce a large change in the carrier density (by more than 10^{14} cm^{-2}) of a FM via electrochemical doping using ionic liquid (IL) gating on functional metal oxides[22]. The mechanism of IL gating is due to the formation and annihilation of oxygen vacancies (V_O)[23, 24]. A gate voltage of 1 V to 5 V applied on the IL is sufficient to induce a drift of V_O in functional oxides, thus achieving the tunability of electrical and magnetic properties of such materials. However, IL usually involves halogen-functional groups and they are corrosive in nature[10].

$La_xSr_{1-x}MnO$ is a family of perovskite manganites which, when optimally doped (x = 1/3), show a metal-insulator transition at temperature (T_c) above 300 K, and they possess a high spin polarization that is favorable for spintronic heteroepitaxial structures[25-29]. Electric field modulation of manganite devices has drawn considerable attention. Wu et.al. reported a shift of Tc by 12 K in a 5 nm thick LSMO channel layer upon electrostatic modulation (charge accumulation/depletion) via FE polarization reversal in $BiFeO_3$ layer[13]. In contrast, Cui et.al. reported a shift of T_c by 70 K in a 15 nm thick LSMO channel layer achieved via electrochemical doping[8]. The large change of T_c in the LSMO channel was attributed to the changing valance ratio of Mn^{4+} and Mn^{3+}, due to V_O movement upon different polarity and magnitude of voltages applied to the LSMO channel.

Here, we report on the use of P(VDF-TrFE) as a medium to induce *Vo* formation/annihilation in a LSMO channel via a series of low voltage pulses. Through structural, electrical and magnetic studies, we demonstrate that the enhancement in the tunability of electrical and magnetic properties of the LSMO channel is caused by the evolution of voltage-induced oxygen ions by pulsed voltages of small amplitude, instead of FE polarization reversal in the P(VDF-TrFE) layer.

Experimental

High quality LSMO thin films of thickness 7.5 nm were grown on (001)-$SrTiO_3$ (STO) substrates by pulsed laser deposition using a KrF excimer laser. Prior to deposition, the substrates were treated with either deionized (DI) water or buffered HF, and then subsequent thermal annealing at 1000 ^oC for 2 hours, in order to obtain clear steps and terraces surfaces[30, 31]. The growth of LSMO was fixed at 700 ^oC at an oxygen pressure of 20 Pa. A post-deposition annealing process was applied *in-situ* at 10 Torr for 5 minutes, and then the samples were cooled down to room temperature at a rate of 10 K/min. The film thickness was controlled by the deposition time based on the calibration rate obtained from a thick sample, and further confirmed with X-Ray Reflectivity (XRR) measurements.

To examine the ionic charge accumulation characteristics of LSMO, field effect devices based on FE polymer of P(VDF-TrFE) deposited on LSMO films were defined into Hall bar structures with 200 μm (20 μm) channel length (width) by photolithography and reactive ion etching (Fig.1a). Au (80 nm)/Ti (15 nm) contact electrodes were prepared by e-beam evaporation. Copolymer of P(VDF-TrFE) with 70/30 mole ratio was dissolved in diethyl carbonate with a mass content of 2.5%. The solution was then spin-coated at 4000 rpm for 30 s on the LSMO film, and was annealed at 120 ^oC in air for two hours to obtain the crystalline structure with ferroelectric β phase. The final thickness of the copolymer film

was 250 nm. Finally, Au (30 nm)/Al (100 nm) top gate electrodes were evaporated through a stainless steel shadow mask (Fig. 1a). The LSMO channel resistance along the longitudinal direction (R_{xx}) was measured with a four point technique at 300 K with a current of 1 μA.

Results and Discussions

Before investigating the LSMO/P(VDF-TrFE) heterostructure, the surface morphology of epitaxial LSMO films was characterized by atomic force microscopy (AFM). Fig. 1b shows the AFM image of a 7.5 nm thick LSMO film, which exhibits atomically flat terraces with widths of a few hundred nm. The step height between terraces is ~ 4 Å, consistent with the unit cell height of LSMO along (001) orientation. The crystallinity of the P(VDF-TrFE)/LSMO heterostructures was examined using a high resolution Rigaku Smartlab system. For relative thick (24 nm) LSMO film (Fig. 1c) thickness fringes alongside the (002) crystallographic plane were observed, implying a highly ordered crystalline structure in the film with a flat surface. When the thickness of the LSMO layer decreases to 7.5 nm, the (002) crystallographic plane of LSMO peak broadens and it is shadowed by the (002) STO peak[32, 33]. On the other hand, the peak at $2\theta = 19.7^{o}$ corresponds to the (100) and (200) crystallographic planes of P(VDF-TrFE) in the ferroelectric β phase[34].

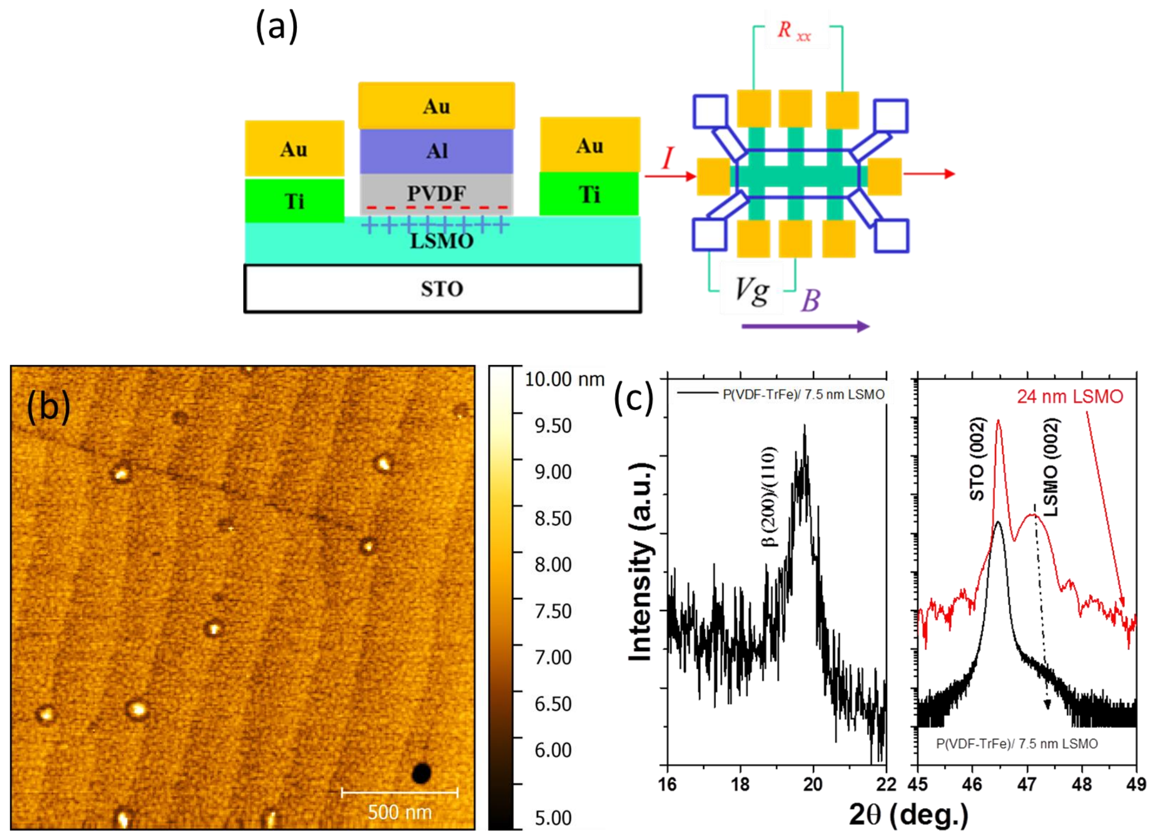

Fig. 1 (a) Schematic illustrations of the device for resistance modulation in LSMO induced by charge accumulation in P(VDF-TrFE) (left), and the Hall bar pattern of the LSMO/P(VDF-TrFE) heterostructure (right). (b) AFM image of a 7.5 nm thick LSMO film grown on TiO_2-terminated STO (001) substrate. (c) XRD pattern of P(VDF-TrFE) /LSMO on STO (001) substrate.

The ferroelectric properties of the heterostructures were examined by piezoelectric force microscope (PFM) measurements. First, the out-of-plane piezoelectric response of the P(VDF-TrFE) grown on LSMO film was measured at room temperature. Fig. 2a shows a clear hysteresis behavior of the PFM phase and amplitude signals, which is acquired by applying a voltage between the PFM tip (positive terminal) in contact with P(VDF-TrFE) and

the LSMO bottom electrode (negative terminal). Good ferroelectric switching is observed, and the phase angle of the PFM signals indicates a nearly 180° polarization switching in the P(VDF-TrFE) layer resulting in the P+ and P- orientation, respectively. Voltage pulses of ±35 V are sufficient for a full switch of the direction of polarization. In addition, ferroelectric switching with low voltage pulses was also examined. Fig. 2b shows the PFM image of the copolymer with regions undergone different poling conditions. The unpoled region (large square) indicates random dipole arrangement, which results in a low piezoelectric signal and noisy PFM phase signals. The intermediate and inner square regions correspond to areas scanned with -10 V and +10 V tip voltage before the PFM scanning. A good ferroelectric phase signal contrast is observed between the inner and intermediate square areas. This shows that a voltage of 10 V applied to the P(VDF-TrFE) film is enough to partially switch the ferroelectric polarization in P(VDF-TrFE). The surface morphology of the copolymer layer acquired during the PFM measurement indicates no surface deformation during the film poling process (Fig. 2c). The presence of the thick P(VDF-TrFE) film concealed the smooth flat terrace steps of LSMO.

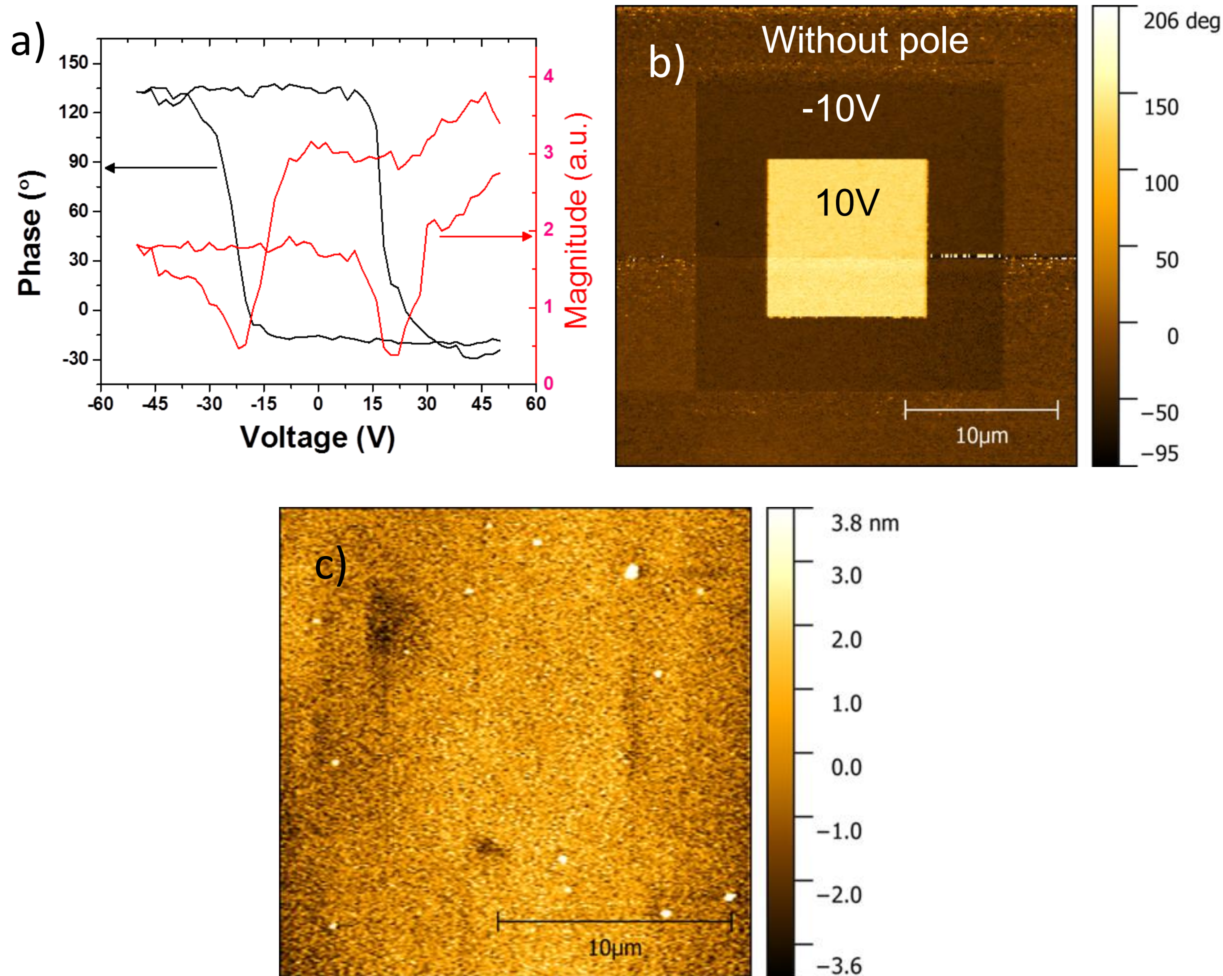

Figure 2 (a) Hysteresis behavior of the PFM signal and phase measured on P(VDF-TrFE) on LSMO film. (b) PFM phase image of a square area with downward and a smaller square inside with upward polarization written with ±10 V. No voltage had been applied to the region outside of the larger square. (c) Surface morphology of a LSMO/P(VDF-TrFE) heterostructure after the PFM scan.

Tunable electrical and magnetic properties of the heterostructure were investigated by measuring the temperature dependence of LSMO channel resistance with upward/downward FE polarization in the P(VDF-TrFE) layer (Fig. 3). A single pulse of 35 V with different polarity leads to FE polarization reversal in the copolymer layer, resulting in a 15 %

resistance change in LSMO channel layer at 300 K, and less than 1% change at 20 K. The drastic decrease in the resistance modulation at low temperature can be attributed to the high carrier concentration in the LSMO layer (~10^{21} cm^3) in the low temperature regime. The resistance change in LSMO layer is induced by the FE polarization of the P(VDF-TrFE) layer. As temperature goes down from 300 K, the screening depth of the polarization of the P(VDF-TrFE) layer becomes more confined to the copolymer/LSMO interface. Since the LSMO channel will undergo a metal to insulator transition at 240 K (characterized by the peak in the resistance-temperature (*R-T)* plot), the screening depth will decrease, resulting in a reduced change of the channel resistance in the low temperature regime [18].

Although a 15 % resistance change is observed in the LSMO layer at 290 K, only a slight shift of the peak in the *R-T* plot of the LSMO channel layer is observed. This tiny shift in *Tc* reflects the dependence between T_C and the carrier concentration in the LSMO channel layer. Under application of +35 V (-35 V) gate voltage, the LSMO channel resistance is increased (decreased) since the hole charge carriers are expelled from (attracted towards) the surface of the LSMO channel layer due to the FE polarization direction of P(VDF-TrFE). This process becomes irreversible if the voltage pulse applied for polarization reversal in P(VDF-TrFE) is too large, as an electric breakdown in the P(VDF-TrFE) layer (at ~400 MV/m) leads to an excess leakage current[35]. Lu et al. demonstrated that the electric field from the surface polarization of ferroelectric oxide BTO can only penetrate through about 2-3 unit-cells (u.c.) (~ 1.2 nm) of the LSMO film[18]. In our case, the field effect from P(VDF-TrFE) in the LSMO channel is expected to be lower than from BTO, since the remnant polarization of BTO (P~45 $\mu C/cm^2$) is much higher than of P(VDF-TrFE) (P~±10 $\mu C/cm^2$).

Wu et al. suggested that the insignificant change of T_c in the manganite channel during the FE polarization reversal is due to inhomogeneous phase separation between FE and FM interfaces[9, 10]. This inhomogeneous phase region, commonly called a dead layer, is composed

of nanoscale metallic (insulating) clusters in the insulating (metallic) matrix when the ferroelectric polarization of P(VDF-TrFE) is pointing upward (downward). The inhomogeneous phase separation in the LSMO channel layer would lead to a change in the channel resistance upon ferroelectric polarization reversal, but with insignificant change of T_C in the manganite.

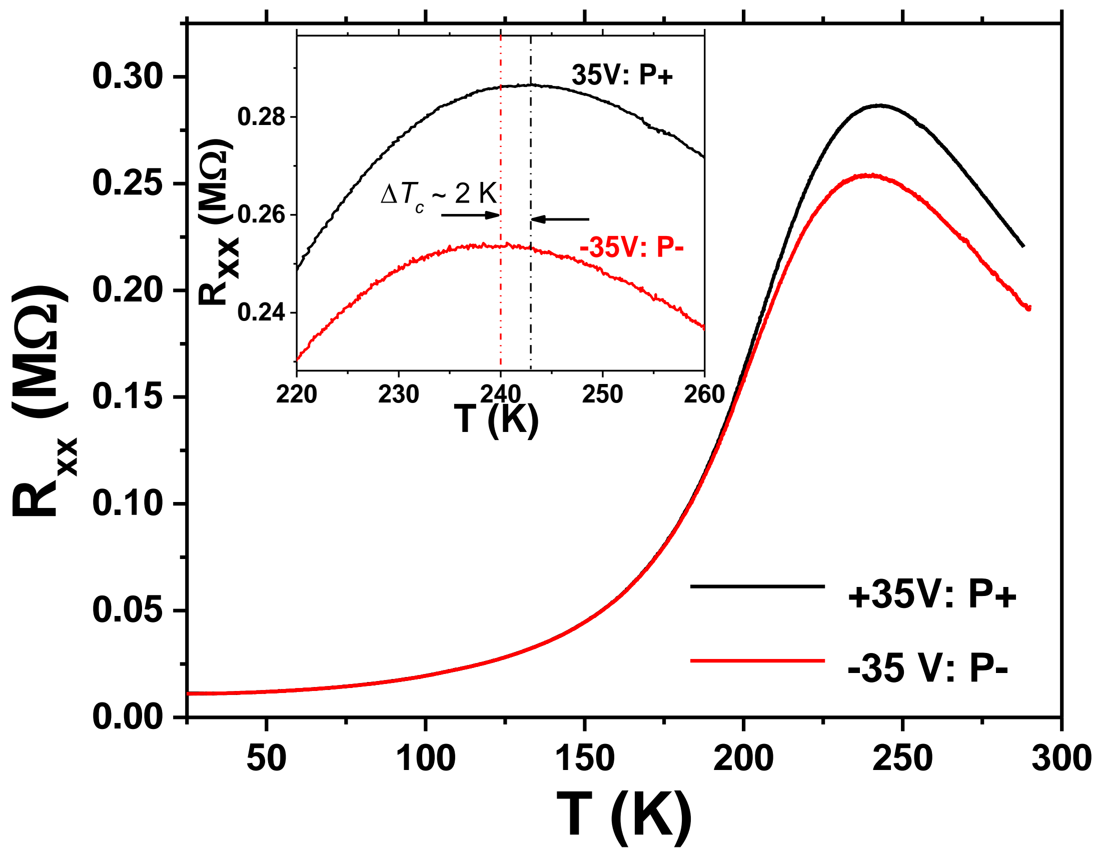

Figure 3. Temperature dependence of the LSMO channel resistance R_{xx} at different ferroelectric polarization (+35V: P+, -35V: P-).

We argue here that the insignificant change of T_c upon ferroelectric polarization reversal is due to the short electrostatics screening depth in the LSMO layer The relative change in T_c due to the resistance change in LMSO channel can be expressed by following equations[36],

$$\Delta T_c \propto \frac{\Delta R}{R} \propto \frac{\Delta n}{n}$$

while Δn can be expressed as,

$$\Delta n \propto \frac{P_r}{d}$$

P_r is the remnant polarization of the FE layer, n is the carrier concentration of LSMO layer and d is the thickness of LSMO layer. Therefore

$$\Delta T_c \propto \frac{P_r}{d}$$

Based on this relation, we deduce that ΔT_c in our case (using the remnant polarization of P(VDF-TrFE) ~ 10 μC/cm^2) should be around 1 K[34], which is consistent with our experimental result. Cui et al. reported that a shift of T_C by 5 K can be obtained in BTO/LSMO heterostructures[37], where the thickness of LSMO layer is 20 u.c. and the remnant polarization of BTO is 48 μC/cm^2.

Alternatively, we also examined the electric field-driven oxygen ion migration in the LSMO channel layer, with the assistance by the dielectric P(VDF-TrFE) layer. Rather than giving a single large pulse for switching the polarization of the FE copolymer, a chain of low voltage pulses (10 V magnitude with 300 ms pulse width at 1.25 Hz) was applied. The LSMO channel layer demonstrates a gradually increasing channel resistance as shown in Fig. 4a. Moreover, the channel resistance is found to remain in the high resistance state after the top gate voltage is removed. The change in channel resistance can be due to the accumulation of

hole carriers (electron depletion) arising from the ferroelectric polarization reversal[9], or it can occur as a result of V_O formation (V_O annihilation) in the LSMO film[38].

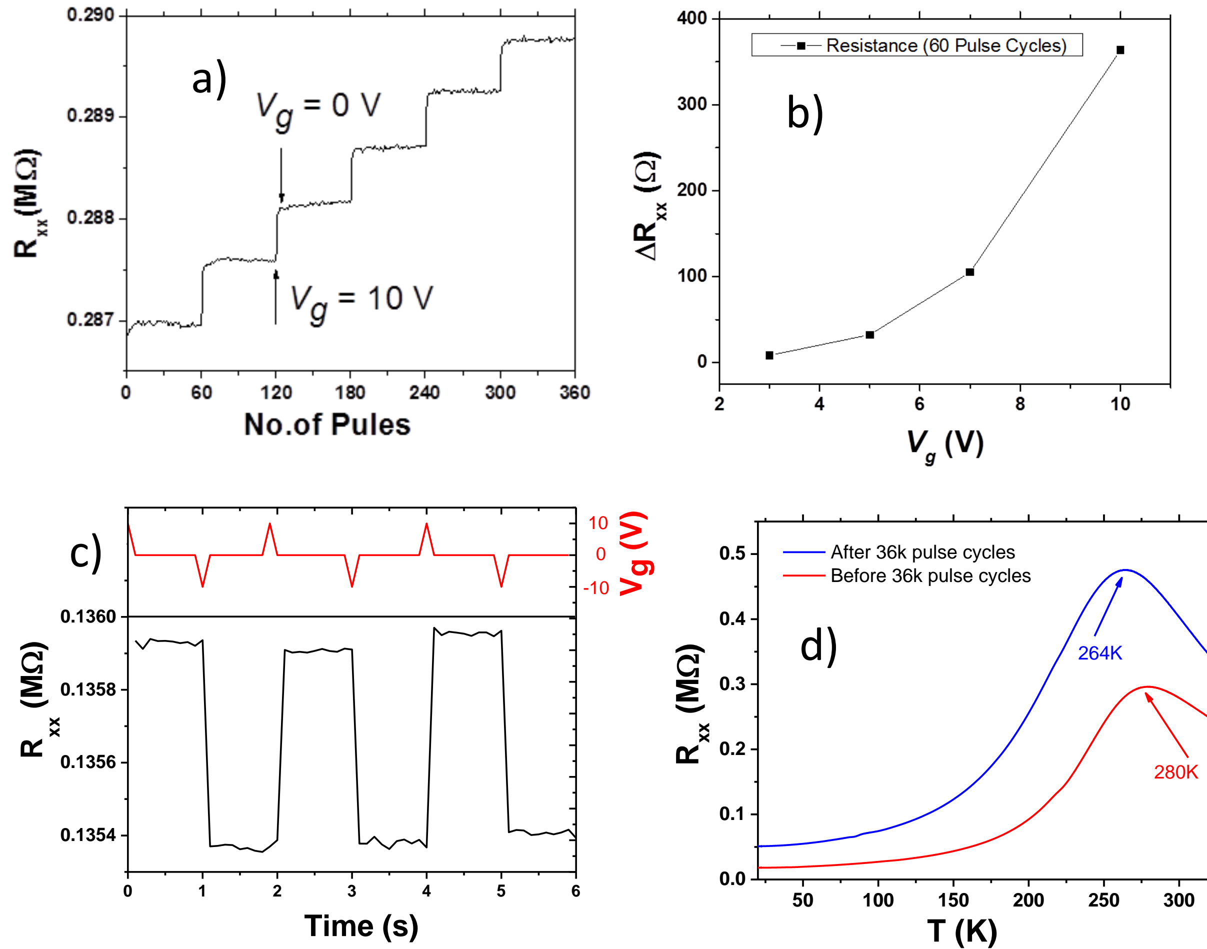

Figure 4. a) Channel resistance R_{xx} upon application of a series of voltage pulses of amplitude 10V. b) Change ΔR_{xx} of the channel resistance upon application of 60 pulse cycles of different amplitude V_g. c) Channel resistance R_{xx} upon application of pulses of ±10 V to the P(VDF-TrFE) layer d) Channel resistance measured over temperature before and after application of 36,000 pulse cycles.

Further evidence of V_O formation or annihilation is seen in the LSMO channel resistance shown in Fig.4b. The application of a continuous chain of 60 pulses with magnitude 5 V (smaller than the coercive field for ferroelectric polarization switching) leads to a change of the channel resistance by more than 30 Ω. By gradually increasing the magnitude of the voltage in the pulse chains from 1 to 10 V, the channel resistance is exponentially increased from 30 to 350 Ω. This increase of the voltage amplitude of the pulses at the gate will generate more V_O at the interface between the P(VDF-TrFE) and LSMO channel layers. Continuous pulses of relatively low gate voltage are sufficient to accumulate the V_O at the LSMO interfaces, since the enthalpy of V_O formation is low[38, 39]. Moreover, the leakage current through the P(VDF-TrFE) gate insulator (400 μm by 500 μm in size) is only 10^{-7} A at 10 V. With such a low leakage current, we believe that the movement of V_O in the LSMO interface is mainly driven by the electric field. The channel resistance R_{xx} controlled via a continuous pulse chain of magnitude ±10 V is shown in Fig. 4c. The two resistance states of the LSMO channel demonstrate that the movement of V_O can be manifested by different polarity of the voltage pulse.

R-T measurements were carried out to investigate the electrical and magnetic properties of the LSMO channel before and after the application of the V_g pulse chain. As presented in Fig. 4d, R_{xx} increases from 0.28 to 0.41 MΩ after 36,000 pulse cycles at 300 K. A three-fold increase of resistance is observed in the low temperature regime. Moreover, T_C of the LSMO channel is shifted down by 14 K after the application of the V_g pulse chain. These observations are attributed to the accumulation of V_O at the LSMO interfaces[40]. As the number of pulses is increased, more and more V_O are formed. These regions of high V_O concentrations in the LSMO interface would lead to a high channel resistance, and a decrease of *Tc* in the LSMO channel layer due to the *p*-type nature of LSMO[8].

We believe that the enhanced tunability of *Tc* with a chain of low voltage pulses is mainly due to V_O formation/annihilation, rather than a result of the FE polarization reversal in P(VDF-TrFE). A gate voltage of ±10 V is not sufficient to switch the polarization of the P(VDF-TrFE) layer completely, as the coercive voltage is ±35 V. Fig. 1a shows that an electric field of ± 10 V can only contribute to a partial change of the phase of the PFM response of the ferroelectric copolymer (a 180° phase change of the PFM signal corresponds to a full switch of the remnant polarization P ~ ±10 μC/cm^2 in the P(VDF-TrFE) layer) [41]. According to the previously discussed relationship between Δ*Tc* and the ferroelectric polarization, an electric field of ±10 V (which leads to 20° phase change out of possible 180°) can only contribute to a change of ΔT_c ~ 0.4 K.

Comparing with the switching by ferroelectric polarization reversal, a continuous and pulsed V_g application to the LSMO channel can offer an enhanced LSMO channel resistance change and tunable capability in T_C. Our results clearly show that field-assisted injection and removal of *Vo* into the LSMO layer can effectively improve the tunability of the LSMO channel, since the density of *Vo* around the LSMO interface is gradually increased and it becomes more and more insulating upon a chain of positive pulsed voltage.

Conclusion

In conclusion, we reported the electric field control of electrical and magnetic properties of a P(VDF-TrFE)/LSMO heterostructure via ferroelectric polarization reversal, as well as by the field-assisted movement of *Vo* through the interface between LSMO and P(VDF-TrFE). With the polarization reversal in the ferroelectric copolymer achieved by the application of single and large electric pulses, a channel resistance change of 15% was observed, accompanied by an insignificant change of *Tc*. In contrast the movement of *Vo* via a successive chain of low-voltage pulses led to a remarkable change of the LSMO channel resistance by 45 %, and a

strong shift of T_C by more than 14 K. Such a low electric field-induced switching effect has the potential to enhance the field-induced magnetism in artificial multiferroic heterostructures.

Acknowledgements

Y.K. Liu acknowledges the financial support from the Natural Science Foundation of China (Grant No.51502129). C.W. Leung acknowledges the financial support of the Hong Kong Research Grant Council (PolyU 153015/14P) and The Hong Kong Polytechnic University (1-ZE25).

References

1. D. C. Ralph and M. D. Stiles, Journal of Magnetism and Magnetic Materials **320** (7), 1190-1216 (2008).
2. M. Bibes and A. Barthelemy, Nat Mater **7** (6), 425-426 (2008).
3. J. Ma, J. Hu, Z. Li and C.-W. Nan, Advanced Materials **23** (9), 1062-1087 (2011).
4. F. Matsukura, Y. Tokura and H. Ohno, Nat Nano **10** (3), 209-220 (2015).
5. S. Fusil, V. Garcia, A. Barthélémy and M. Bibes, Annual Review of Materials Research **44** (1), 91-116 (2014).
6. W. P. Zhou, Q. Li, Y. Q. Xiong, Q. M. Zhang, D. H. Wang, Q. Q. Cao, L. Y. Lv and Y. W. Du, Scientific Reports **4**, 6991 (2014).
7. H. Ohno, D. Chiba, F. Matsukura, T. Omiya, E. Abe, T. Dietl, Y. Ohno and K. Ohtani, Nature **408** (6815), 944-946 (2000).
8. B. Cui, C. Song, G. Wang, Y. Yan, J. Peng, J. Miao, H. Mao, F. Li, C. Chen, F. Zeng and F. Pan, Advanced Functional Materials **24** (46), 7233-7240 (2014).
9. T. Wu, S. B. Ogale, J. E. Garrison, B. Nagaraj, A. Biswas, Z. Chen, R. L. Greene, R. Ramesh, T. Venkatesan and A. J. Millis, Physical Review Letters **86** (26), 5998-6001 (2001).
10. A. S. Dhoot, C. Israel, X. Moya, N. D. Mathur and R. H. Friend, Physical Review Letters **102** (13), 136402 (2009).
11. MaruyamaT, ShiotaY, NozakiT, OhtaK, TodaN, MizuguchiM, A. A. Tulapurkar, ShinjoT, ShiraishiM, MizukamiS, AndoY and SuzukiY, Nat Nano **4** (3), 158-161 (2009).
12. V. Laukhin, V. Skumryev, X. Martí, D. Hrabovsky, F. Sánchez, M. V. García-Cuenca, C. Ferrater, M. Varela, U. Lüders, J. F. Bobo and J. Fontcuberta, Physical Review Letters **97** (22), 227201 (2006).
13. S. M. Wu, S. A. Cybart, D. Yi, J. M. Parker, R. Ramesh and R. C. Dynes, Physical Review Letters **110** (6), 067202 (2013).
14. S. M. Wu, S. A. Cybart, P. Yu, M. D. Rossell, J. X. Zhang, R. Ramesh and R. C. Dynes, Nat Mater **9** (9), 756-761 (2010).
15. P. Silvia and E. Claude, Journal of Physics: Condensed Matter **21** (30), 303201 (2009).
16. C. H. Ahn, J. M. Triscone and J. Mannhart, Nature **424** (6952), 1015-1018 (2003).
17. T. Zhao, S. B. Ogale, S. R. Shinde, R. Ramesh, R. Droopad, J. Yu, K. Eisenbeiser and J. Misewich, Applied Physics Letters **84** (5), 750-752 (2004).
18. H. Lu, T. A. George, Y. Wang, I. Ketsman, J. D. Burton, C.-W. Bark, S. Ryu, D. J. Kim, J. Wang, C. Binek, P. A. Dowben, A. Sokolov, C.-B. Eom, E. Y. Tsymbal and A. Gruverman, Applied Physics Letters **100** (23), 232904 (2012).
19. A. J. Lovinger, Science **220** (4602), 1115-1121 (1983).
20. Q.-D. Ling, D.-J. Liaw, C. Zhu, D. S.-H. Chan, E.-T. Kang and K.-G. Neoh, Progress in Polymer Science **33** (10), 917-978 (2008).
21. I. Stolichnov, S. W. E. Riester, H. J. Trodahl, N. Setter, A. W. Rushforth, K. W. Edmonds, R. P. Campion, C. T. Foxon, B. L. Gallagher and T. Jungwirth, Nat Mater **7** (6), 464-467 (2008).
22. H. Yuan, H. Shimotani, A. Tsukazaki, A. Ohtomo, M. Kawasaki and Y. Iwasa, Advanced Functional Materials **19** (7), 1046-1053 (2009).
23. K. Fujiwara, T. Ichimura and H. Tanaka, Advanced Materials Interfaces **1** (3), n/a-n/a (2014).
24. H. T. Yi, B. Gao, W. Xie, S.-W. Cheong and V. Podzorov, Scientific Reports **4**, 6604 (2014).
25. H. K. Lau and C. W. Leung, J. Appl. Phys. **104**, 123705 (2008).
26. A. Ruotolo, C. W. Leung, C. Y. Lam, W. F. Cheng, K. H. Wong and G. P. Pepe, Physical Review B **77** (23), 233103 (2008).
27. A. Ruotolo, C. Y. Lam, W. F. Cheng, K. H. Wong and C. W. Leung, Physical Review B **76** (7), 075122 (2007).
28. H. F. Wong, K. Wang, C. W. Leung and K. H. Wong, IEEE Transactions on Magnetics **50** (7), 1-4 (2014).

29. A. Urushibara, Y. Moritomo, T. Arima, A. Asamitsu, G. Kido and Y. Tokura, Physical Review B **51** (20), 14103-14109 (1995).
30. J. G. Connell, B. J. Isaac, G. B. Ekanayake, D. R. Strachan and S. S. A. Seo, Applied Physics Letters **101** (25), 251607 (2012).
31. M. Kawasaki, K. Takahashi, T. Maeda, R. Tsuchiya, M. Shinohara, O. Ishiyama, T. Yonezawa, M. Yoshimoto and H. Koinuma, Science **266** (5190), 1540-1542 (1994).
32. W. Yuan, Y. Zhao, C. Tang, T. Su, Q. Song, J. Shi and W. Han, Applied Physics Letters **107** (2), 022404 (2015).
33. M. Huijben, P. Yu, L. W. Martin, H. J. A. Molegraaf, Y. H. Chu, M. B. Holcomb, N. Balke, G. Rijnders and R. Ramesh, Advanced Materials **25** (34), 4739-4745 (2013).
34. W. J. Hu, D.-M. Juo, L. You, J. Wang, Y.-C. Chen, Y.-H. Chu and T. Wu, Scientific Reports **4**, 4772 (2014).
35. B. Chu, X. Zhou, K. Ren, B. Neese, M. Lin, Q. Wang, F. Bauer and Q. M. Zhang, Science **313** (5785), 334-336 (2006).
36. T. Kanki, Y.-G. Park, H. Tanaka and T. Kawai, Applied Physics Letters **83** (23), 4860-4862 (2003).
37. B. Cui, C. Song, H. Mao, H. Wu, F. Li, J. Peng, G. Wang, F. Zeng and F. Pan, Advanced Materials **27** (42), 6651-6656 (2015).
38. J. Walter, H. Wang, B. Luo, C. D. Frisbie and C. Leighton, ACS Nano **10** (8), 7799-7810 (2016).
39. G. H. Jonker and J. H. Van Santen, Physica **19**, 120−130 (1953).
40. Y. B. Nian, J. Strozier, N. J. Wu, X. Chen and A. Ignatiev, Physical Review Letters **98** (14), 146403 (2007).
41. W. Zhang, M.-M. Yang, X. Liang, H.-W. Zheng, Y. Wang, W.-X. Gao, G.-L. Yuan, W.-F. Zhang, X.-G. Li, H.-S. Luo and R.-K. Zheng, Nano Energy **18**, 315-324 (2015).